Journal of Organometallic Chemistry 693 (2008) 3411–3418

Contents lists available at ScienceDirect

Journal of Organometallic Chemistry

journal homepage: www.elsevier.com/locate/jorganchem

Nitrogen donor ligands bearing N–H groups: Effect on catalytic and cytotoxic activity of molybdenum η^3-allyldicarbonyl complexes

Marta S. Saraiva [a], Susana Quintal [a], Fátima C.M. Portugal [a], Telma A. Lopes [a], Vitor Félix [b], José M.F. Nogueira [a], Margarida Meireles [a], Michael G.B. Drew [c], Maria José Calhorda [a,*]

[a] Universidade de Lisboa, Faculdade de Ciências, Departamento de Química e Bioquímica e Centro de Química e Bioquímica, Campo Grande, 1749-016 Lisboa, Portugal
[b] Departamento de Química, CICECO, Universidade de Aveiro, 3810-193 Aveiro, Portugal
[c] School of Chemistry, University of Reading, Whiteknights, Reading RG6 6AD, UK

ARTICLE INFO

Article history:
Received 28 May 2008
Received in revised form 30 July 2008
Accepted 4 August 2008
Available online 11 August 2008

Keywords:
Molybdenum(II) complexes
Cytotoxic activity
Carbonyl
Diimines
Catalysis
Olefin epoxidation

ABSTRACT

Reactions of $[Mo(\eta^3\text{-}C_3H_5)Br(CO)_2(NCMe)_2]$ with the bidentate nitrogen ligands 2-(2′-pyridyl)imidazole (**L1**), 2-(2′-pyridyl)benzimidazole (**L2**), *N*,*N*′-bis(2′-pyridinecarboxamido)-1,2-ethane (**L3**), and 2,2′-bisimidazole (**L4**) led to the new complexes $[Mo(\eta^3\text{-}C_3H_5)Br(CO)_2(L)]$ (L = **L1**, **1**; **L2**, **2**; **L4, 4**) and $[\{Mo(\eta^3\text{-}C_3H_5)Br(CO)_2\}_2(\mu\text{-}\mathbf{L3})]$ (**3**).

The reaction of complexes **2** and **3** with $Tl[CF_3SO_3]$ afforded $[Mo(\eta^3\text{-}C_3H_5)(CF_3SO_3)(CO)_2(\mathbf{L2})]$ (**2T**) and $[\{Mo(\eta^3\text{-}C_3H_5)(CF_3SO_3)(CO)_2\}_2(\mu\text{-}\mathbf{L3})]$ (**3T**).

Complexes **3** and **2T** were structurally characterized by single crystal X-ray diffraction, showing the facial allyl/carbonyls arrangement and the formation of the axial isomer. In **2T**, two molecules are assembled in a hydrogen bond dimer.

The four complexes **1–4** were tested as precursors in the catalytic epoxidation of cyclooctene and styrene, in the presence of *t*-butylhydroperoxide (TBHP), with moderate conversions and turnover frequencies for complexes **1–3** and very low ones for **4**. The increasing number of N–H groups in the complexes seems to be responsible for the loss of catalytic activity, compared with other related systems. The cytotoxic activities of all the complexes were evaluated against HeLa cells. The results showed that compounds **1, 2, 4**, and **2T** exhibited significant activity, complexes **2** and **2T** being particularly promising.

1. Introduction

Organometallic complexes play a major role in many fields of chemistry, as precursors to new materials [1], in applications to medicine [2], and in catalysis [3], among others. Their versatility is associated with the possibility of finely tuning the stereoelectronic properties of metal centers by changing ligands, oxidation state and electron configuration. These properties explain their large use as homogeneous catalysts for the production of chemicals [4], while their immobilization in selected supports aims at bringing together the advantages of heterogeneous catalysts (product separation and catalyst recovery) with the usual high selectivity of homogeneous catalysts. The family of η^3-allyldicarbonyl complexes of Mo(II), and to a smaller extent W(II), has been widely studied in coordination chemistry and catalysis [5], since they couple an easy synthetic procedure to the possibility of introducing a variety of ligands. The complex $[Mo(\eta^3\text{-allyl})X(CO)_2(NCMe)_2]$ (X = halide) [6], in particular, is a very useful precursor, as both the nitriles and X can be substituted by neutral or anionic ligands, to yield complexes displaying catalytic activity in a large range of reactions. Imine aziridination [7], oxidation of triphenylphosphine with molecular oxygen [8], or allylic alkylations [9], are examples of such reactivity. The nitrile complexes $[Mo(\eta^3\text{-}C_3H_5)X(CO)_2(NCMe)_2]$ have been shown to act as precursors in the ring-opening metathesis polymerization of norbornene [10] and polymerization of terminal acetylenes as well as catalyze the oligomerization of Ph(C≡C)Ph, *n* = (1, 2) [11]. In a recent work, it was found that both $[Mo(\eta^3\text{-}C_3H_5)X(CO)_2(NCMe)_2]$ (X = Cl, Br) and some of their 1,4-diaza-1,3-butadienes derivatives behave as precursors in selective olefin epoxidation in the presence of *t*-butyl hydroperoxide (TBHP) [12]. Molybdenum complexes are known for their industrial applications in homogeneous olefin epoxidation, such as the ARCO-Halcon process, where TBHP is the source of oxygen [13]. Although it is well known that Mo(VI) species are the active species in oxidation catalysis, several Mo(II) systems, such as $MoCpCl(CO)_3$ ($Cp = \eta^5\text{-}C_5H_5$), are oxidized by TBHP to dioxo Mo(VI) complexes, which in turn catalyze olefin epoxidation [14]. The carbonyl complexes can be used directly, as the formation of the active species is not rate determining in the whole catalytic process [14c]. The turnover frequencies can reach values such as high as 21 000 mol mol_{Mo}^{-1} h^{-1} obtained by the well-known epoxidation

* Corresponding author. Tel.: +351 217 500 196; fax: +351 217 500 088.
E-mail address: mjc@fc.ul.pt (M.J. Calhorda).

0022-328X/$ - see front matter © 2008 Elsevier B.V. All rights reserved.
doi:10.1016/j.jorganchem.2008.08.001

catalyst $MeReO_3/H_2O_2$ [15]. We found that [Mo(η^3-C_3H_5)X$(CO)_2$(N)$_2$] (X = Cl, Br; N = NCMe or N_2=1,4-diaza-1,3-butadienes) were even better precursors in the same reaction, leading to similar conversions and turnover frequencies, and exhibiting a high activity in the second run [12]. Chloride derivatives were more active than the bromide analogues, but the details of the mechanism and the exact role of the nitrogen ligands are not yet clear.

Following these results and our interest in the chemistry of the η^3-allyldicarbonyl molybdenum(II) fragment [16], we prepared and characterized new complexes of the type [Mo(η^3-allyl)Br$(CO)_2$(N-N)], where some of the dinitrogen ligands are unsymmetrical molecules, and tested their activity as precursors for the catalytic epoxidation of olefins using TBHP. Since some related Mo(II) complexes displayed antitumoral activity *in vitro* [17], the biological activity of the new complexes was studied on HeLa cells.

2. Results and discussion

2.1. [Mo(η^3-C_3H_5)Br$(CO)_2$(L)] and [{Mo(η^3-C_3H_5)Br$(CO)_2$}$_2$(μ-L)] complexes

The dinitrogen ligands 2-(2′-pyridyl)imidazole (**L1**), 2-(2′-pyridyl)benzimidazole (**L2**), *N*,*N*′-bis(2′-pyridinecarboxamido)-1,2-ethane (**L3**), and 2,2′-bisimidazole (**L4**) are sketched in Scheme 1. The complexes [Mo(η^3-C_3H_5)Br$(CO)_2$(L)] (L = **L1**, **1**; **L2**, **2**; **L4, 4**) and [{Mo(η^3-C_3H_5)Br$(CO)_2$}$_2$(μ-**L3**)] (**3**) were prepared by reaction between each ligand and the precursor [Mo(η^3-C_3H_5)X$(CO)_2$(NCMe)$_2$] (**5**), in 1:1 ratio (**L1**, **L2**, **L4**) or 1:2 for **L3**, in dichloromethane (Scheme 2). They were characterized by elemental analysis, FTIR and ^{1}H and ^{13}C NMR spectroscopy. Complex **3** was also structurally characterized by single crystal X-ray diffraction.

The two more stable isomers of this type of complexes are shown in Scheme 3: the axial (left), without any symmetry element, and the equatorial (right), which may have a mirror plane when the ligand is symmetrical, as happens with **L4** after coordination. They may interconvert in solution and there is not a clear preference for one of them, as has been shown by several experimental and computational studies [16,18]. When the bidentate ligand is bulky, the axial isomer tends to be favored, and sometimes there is no fluxionality in solution.

The $\nu_{C\equiv O}$ stretching modes of the *cis*-C≡O groups are observed at 1933 and 1839 cm^{-1} (**1**), 1934 and 1853 cm^{-1} (**2**), 1928 and 1824 cm^{-1} (**3**), 1930 and 1832 cm^{-1} (**4**), slightly shifted from 1944 and 1850 cm^{-1} in the parent complex **5**. Complex **3** with a N, O ligand exhibits the largest deviations. The $\nu_{C=O}$ mode change from 1656 cm^{-1} in the free ligand **L3** to 1630 cm^{-1} in complex **3**, indicating the coordination of the C=O group to molybdenum. The coordination of the ligands is also reflected in the $\nu_{C=N}$ and ν_{N-H} frequencies. The $\nu_{C=N}$ vibrational modes shift to lower wavenumbers upon coordination, from 1689 and 1594 cm^{-1} (**L1**), 1569 and 1598 cm^{-1} (**L2**), 1656 cm^{-1} (**L3**), 1545 cm^{-1} (**L4**) in the free ligands to 1616 and 1547 cm^{-1} (**1**), 1539 and 1602 cm^{-1} (**2**), 1600 cm^{-1} (**3**), 1528 cm^{-1} (**L4**) in the complexes. The N–H stretching frequency varies significantly from ligand **L3** (3331 cm^{-1}) where two N–H···N hydrogen bonds can occur, to the complex where they disappear after the coordination of the pyridine nitrogen atoms (3264 cm^{-1}); changes are smaller in the other compounds.

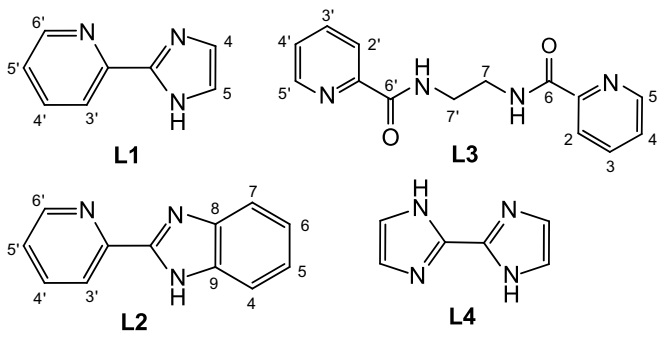

Scheme 1.

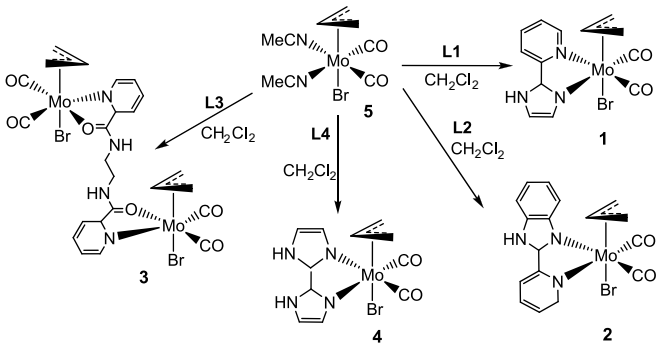

Scheme 2.

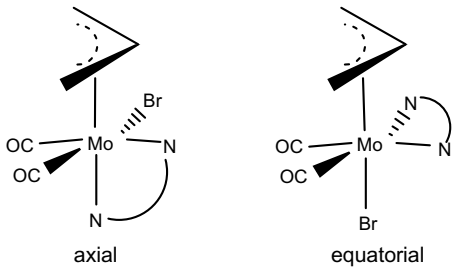

Scheme 3.

^{1}H and ^{13}C NMR spectra were taken and HMQC experiments were performed to interpret and assign them. It should be reminded that in the axial isomer the five allylic protons should always be non equivalent. On the other hand, in the equatorial isomer, a symmetric ligand such as bisimidazole (**L4**) should lead to three allylic peaks, as the *syn* and the *anti* protons are equivalent. This no longer holds for asymmetric ligands such as **L1–L3**. The ^{1}H NMR spectra of the complexes show the peaks of the coordinated ligands in **L1–L4** shifted relative to those of the free ligands. For instance, in the spectrum of complex **1**, [Mo(η^3-C_3H_5)Br$(CO)_2$(**L1**)] only one peak assigned to the H_{meso} is observed (quintet, 4.10 ppm); two very close doublets appear at around 3.60 ppm for the H_{syn}, while the two H_{anti} protons are more separated (1.43 and 1.58 ppm). Only one isomer is observed in MeOD solution. The **L1** ligand signals shift, namely H4 and H5 from 7.18 and 7.11 ppm, respectively, in the free ligand to 7.60 ppm in complex **1**. The peaks assigned to H6′, H3′, H4′, and H5′ shift from 8.50, 8.18, 7.78, 7.26 in **L1** to 8.28, 8.11, 7.98, and 7.79 ppm in **1**. The ^{13}C NMR spectra of ligand **L1** and complex **1** also allow the assignment of peaks (see Section 4).

High-resolution mass spectra (HR-MS) were acquired using the electrospray ionization (ESI) technique to confirm the proposed structure of ligand **L3** and complexes **3** and **4**. Both the molecular mass and the isotopic pattern were analyzed. **L3** was successfully detected as a potassium adduct at m/z = 309.07563, with an error of 2.6 ppm for the expected formula of [**L3**+K]$^+$ (m/z = 309.07483). For both complexes **3** and **4**, although the ESI method used is very mild, it was not possible to confirm the masses as for-

mulated in Scheme 2. The detected m/z peaks corresponded in both cases to the desired complexes with the loss of the Br ligand. In this way complex **3** was detected as $[\mathbf{3}-Br]^+$ at $m/z = 738.90328$, with an error of 2.2 ppm, relative to the calculated $m/z = 738.89824$. For complex **4** the peak detected at $m/z = 328.99579$ for $[\mathbf{4}-Br]^+$ had an error of 9.4 ppm relative to the expected $m/z = 328.99322$. The isotopic pattern match was complete for all species.

2.2. $[\{Mo(\eta^3\text{-}C_3H_5)(CF_3SO_3)(CO)_2\}_n(\mathbf{L})]$ (n = 1,2) complexes

The reaction between the complexes **1–4** and $Tl[CF_3SO_3]$ in acetonitrile was studied and was successful when using complexes **2** and **3**, containing the ligands 2-(2′-pyridyl)benzimidazole (**L2**) and N,N′-bis(2′-pyridinecarboxamido)-1,2-ethane (**L3**) (Scheme 4).

The coordination of the triflate anion to molybdenum, to form a neutral species, was unambiguously demonstrated by single crystal X-ray diffraction study of complex **2T** (see below).

The FTIR spectra show the vibrations characteristic of the triflate at 1285 ($\nu_{as(SO_3)}$), 1022 ($\nu_{s(SO_3)}$), 1226 ($\nu_{s(CF_3)}$), and 1179 cm^{-1} ($\nu_{as(CF_3)}$) for complex **2T** and at 1291 ($\nu_{as(SO_3)}$), 1030 ($\nu_{s(SO_3)}$), 1225 ($\nu_{s(CF_3)}$), and 1182 cm^{-1} ($\nu_{as(CF_3)}$) for complex **3T**. The similarity between these values suggests that the triflate is associated with molybdenum in the same way in both complexes. The typical $\nu_{C=O}$ stretching modes are only slightly shifted by the substitution of bromide by triflate, being observed at 1948 and 1865 cm^{-1} in complex **2T**, and at 1949 and 1853 cm^{-1} in complex **3T**. Analogous small deviations occur for the other vibrational modes, namely $\nu_{C=N}$ and ν_{N-H}.

The presence of three isomers of **2T** in the ^1H NMR spectrum is detected by the three peaks at 4.25, 3.83, and 3.58 ppm, which may be assigned to the H_{meso} of the allyl ligand. Several peaks correspond to the H_{syn} (2 multiplets at 3.02–3.38 ppm) and the H_{anti} protons (2 doublets at 1.30–1.40 ppm). The peaks of the pyridylbenzimidazole ligand appear in the range 7.56–9.10, with the N–H proton at 8.90 ppm. The ^1H NMR spectrum of complex **3T** is simpler, with a multiplet at 4.17 ppm, assigned to the two equivalent H_{meso} of the two allyl ligands, a doublet at 1.71 ppm (four H_{anti} protons) and two doublets at 3.77 and 3.96 ppm (four H_{syn} protons). The two protons of the C–C (aliphatic) chain appear as a multiplet at 3.69 ppm, the pyridyl protons at 7.83 (H4,4′), 7.88 (H2,2′), 8.03 (H3,3′), and 9.68 (H5,5′), while the N–H protons are observed at 8.91 ppm.

High-resolution mass spectra (HR-MS) were also performed to characterize complex **3T**. As described above, the detected m/z peak corresponded to the desired complex with the loss of one $CF_3SO_3^-$ ligand, at $m/z = 808.94041$. The error found for $[\mathbf{3T}-(CF_3SO_3)]^+$, relative to the calculated $m/z = 808.93318$, was 7.1 ppm.

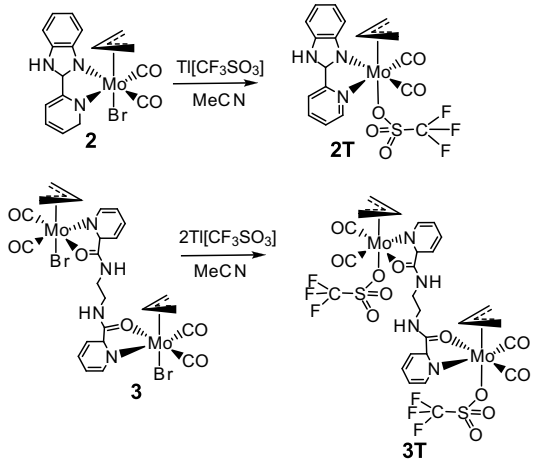

Scheme 4.

2.3. Crystallography

The crystal structure of complexes **3** and **2T** was determined by single crystal X-ray diffraction. Selected bond distances and angles for both complexes are given in Table 1. The molecules found in the solid state are shown in Fig. 1 for **3** and in Fig. 2 for **2T**.

The binuclear complex $[\{Mo(\eta^3\text{-}C_3H_5)Br(CO)_2\}_2(\mu\text{-}\mathbf{L3})]$ (**3**) displays a two fold symmetry with the crystallographic axis bisecting the bridging ligand at the C(19)–C(19)* bond (see Fig. 1, right). The N–H binding groups are hydrogen bonded to the bromine atoms with a N–H···Br distance of 2.61 Å and an angle of 177°. These two intramolecular hydrogen bonds compel the ethylenediamine fragment from the bridging ligand **L3** to adopt a gauche conformation with a N–C–C–N torsion angle of 39.0(9)°. The two molecules of **2T** are self-assembled by two hydrogen bonds between triflate anions and pyridylbenzimidazole ligands with N–H···O distances and corresponding angles of 2.02 Å and 162°. In this crystallographic centrosymmetric arrangement, the pyridylbenzimidazole ligands **L2** are almost planar with an interplanar distance of 3.32 Å. The coordination environment of each molybdenum center is pseudo octahedral with the chelating ligand occupying one equatorial and one axial position, with N–Mo–N bite angles of 72.8(2)° for **2T** and N–Mo–O of 72.6(2)° for **3**. The second axial position is fulfilled with the η^3-allyl ligand and therefore the relative spatial disposition of these ligands is consistent with the formation of axial isomers in both complexes. The monodentate ligands, bromide in **3** and triflate anion in **2T**, lie on the equatorial coordination plane intersecting the plane of the bidentate ligand at 81.2(1)° in **2T** and 74.8(3)° in **3**. This geometric arrangement is comparable to that found in related η^3-allyldicarbonyl molybdenum(II) complexes containing bulky ligands [12,16,19]. The distances and the angles subtended at Mo(II) centers are within the expected values.

2.4. Catalytic epoxidation of olefins

All complexes were tested as catalyst precursors for olefin epoxidation using *cis*-cyclooctene and styrene as substrates and *tert*-butyl hydroperoxide (TBHP in decane) as oxygen donor, in

Table 1
Selected bond distances (Å) and angles (°) in the molybdenum coordination sphere of $[\{Mo(\eta^3\text{-}C_3H_5)Br(CO)_2\}_2(\mu\text{-}\mathbf{L3})]$ (**3**) and $[Mo(\eta^3\text{-}C_3H_5)(CF_3SO_3)(CO)_2(\mathbf{L2})]$ (**2T**)

3			
Mo–C(100)	1.960(11)	Mo–C(200)	1.939(9)
Mo–N(11)	2.245(6)	Mo–O(20)	2.233(5)
Mo–Br	2.729(2)	Mo–C(1)	2.363(10)
Mo–C(2)	2.212(8)	Mo–C(3)	2.333(9)
C(100)–Mo–C(200)	80.6(4)	O(20)–Mo–N(11)	72.6(2)
C(100)–Mo–N(11)	88.1(3)	C(200)–Mo–N(11)	96.7(3)
C(100)–Mo–O(20)	100.0(3)	C(200)–Mo–O(20)	169.2(3)
C(100)–Mo–Br	168.0(3)	C(200)–Mo–Br	95.8(3)
N(11)–Mo–Br	80.9(2)	O(20)–Mo–Br	81.5(1)
2T			
Mo–C(100)	1.936(7)	Mo–C(200)	1.949(7)
Mo–N(11)	2.340(5)	Mo–N(21)	2.206(6)
Mo–O(31)	2.298(4)	Mo–C(1)	2.346(7)
Mo–C(2)	2.206(7)	Mo–C(3)	2.333(7)
C(100)–Mo–C(200)	78.8(3)	N(21)–Mo–N(11)	72.8(2)
N(11)–Mo–O(31)	79.4(2)	N(21)–Mo–O(31)	81.1(2)
C(100)–Mo–O(31)	170.1(2)	C(200)–Mo–O(31)	100.3(2)
C(100)–Mo–N(11)	99.4(2)	C(200)–Mo–N(11)	168.2(2)
C(100)–Mo–N(21)	89.1(2)	C(200)–Mo–N(21)	95.5(2)

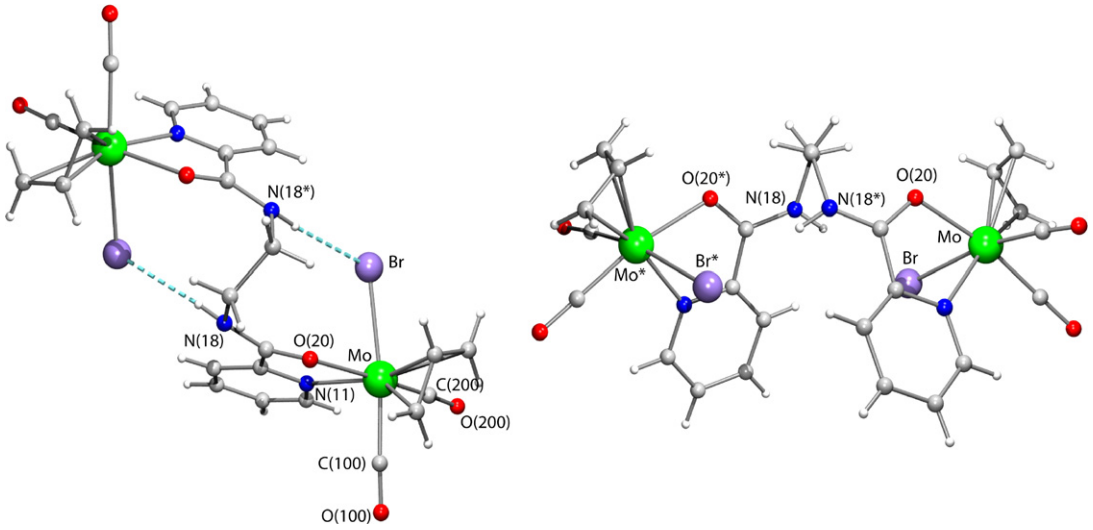

Fig. 1. Molecular structure of [{Mo(η^3-C_3H_5)Br(CO)$_2$}$_2$(μ-**L3**)] (**3**) in two different views showing the axial isomer (left) and the 2-fold crystallographic symmetry (right). $*$ denotes the symmetry operation $-x, y, 0.5 - z$.

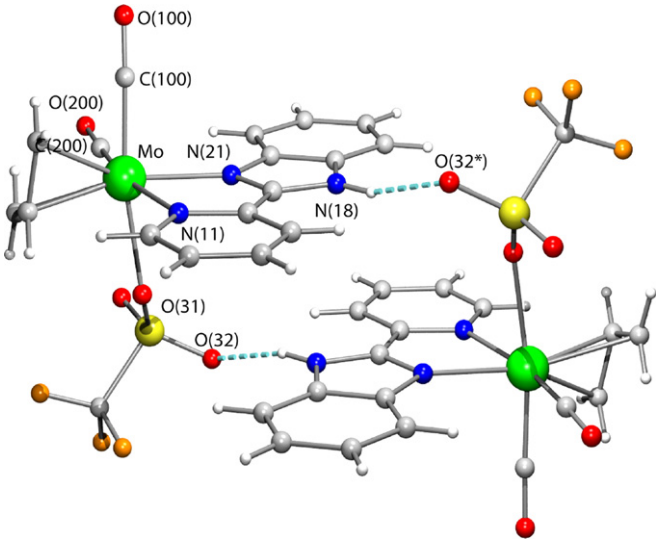

Fig. 2. Molecular structure of [Mo(η^3-C_3H_5)(CF_3SO_3)(CO)$_2$(**L2**)] (**2T**) showing two axial isomers assembled as a dimer.

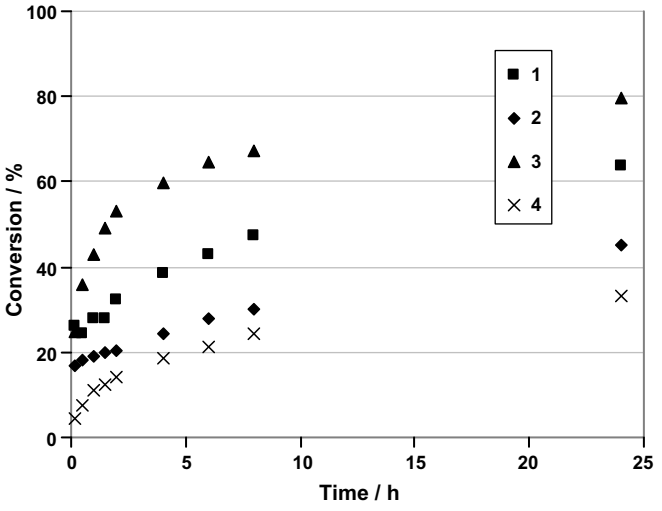

Fig. 3. Conversion of cyclooctene using TBHP as oxygen donor, in the presence of complexes [Mo(η^3-C_3H_5)Br(CO)$_2$(L)] (L = **L1**, **1**; **L2**, **2**; **L4**, **4**) and [{Mo(η^3-C_3H_5)Br(CO)$_2$}$_2$(μ-**L3**)] (**3**).

dichloromethane, at 55 °C (see details in Section 4). Almost no reaction took place in the absence of a catalyst, which was initiated by the addition of a Mo complex (Fig. 3). Only epoxides were detected as the product of the reaction (24 h) when cyclooctene was the substrate. In the oxidation of styrene, some secondary reaction products were detected (see Table 2).

The activity of three of the complex precursors (**1–3**) is very similar, with TOFs slightly higher for oxidation of styrene than of cyclooctene. Conversions are higher for the binuclear complex **3,** as there are two molybdenum atoms per molecule of the catalyst precursor and therefore of the active species. The best TOFs are achieved by complex **1** bearing the small ligand and decrease in complex **2** where there is an extra benzene ring in the ligand. There is practically no induction period for catalyst precursors **1–3**. The activity is very high in the beginning of the reaction and then slows down in a similar way for the three complexes.

On the other hand, complex **4** displays low conversions and very small turnover frequencies for both substrates. In the reaction with styrene, conversion starts to be observed only after a very long induction period of ~6 h.

Table 2
Olefin epoxidation of cyclooctene and styrene, using TBHP as oxygen donor, in the presence of complexes [Mo(η^3-C_3H_5)Br(CO)$_2$(L)] (L = **L1**, **1**; **L2**, **2**; **L4, 4**) and [{Mo(η^3-C_3H_5)Br(CO)$_2$}$_2$(μ-**L3**)] (**3**)

Complex	Substrate	TOF[a] (mol mol$_{Mo}^{-1}$ h^{-1})	Conv.[b] (%)
1	Cyclooctene	159	64
	Styrene	175	54
2	Cyclooctene	101	45
	Styrene	150	52
3	Cyclooctene	75	80
	Styrene	82	90
4	Cyclooctene	29	33
	Styrene	–[c]	24

[a] Turnover frequency calculated at 10 min, at 55 °C.
[b] Cyclooctene conversion after 24 h reaction, at 55 °C.
[c] No conversion in this period.

As discussed in more detail in a previous publication [12], it is believed that the first step in the reaction consists of the oxidation of the Mo(II) precursor to a Mo(VI) species by means of the TBHP oxidant. Other Mo(II) complexes, such as $CpMoX(CO)_3$, can act as efficient precursors, forming the active Mo(VI) species *in situ* [14]. In the course of the reaction, epoxide is produced, with *t*-butanol as a side-product. The formation of alcohol leads to a competition reaction with the active species and this reaction tends to decrease the activity of the catalyst, as has been reported before, and is also observed in the curves of Fig. 3 [20].

The Mo(II) complexes described in this work differ from those previously reported [12] by the bidentate nitrogen ligand and their catalytic performance is not particularly good. The most striking feature of the four ligands is the presence of one or two NH groups. Indeed, complex **4** with two NH groups displays the lowest activity, suggesting that they may interfere with the catalytic cycle by forming hydrogen bonds with TBHP and stabilizing the wrong species. Hydrogen bonds play a role in the proposed mechanism for this reaction and the least active complex **4** has a ligand with two NH bonds. The most active catalyst precursor **1** has the smallest ligand, suggesting that steric effects may be relevant in this system.

2.5. Biological studies

Preliminary studies on the cytotoxicity of compounds were carried out on HeLa cells (human cancer strain), using the colorimetric mitochondrial function-based MTT viability assay. The IC_{50} values were calculated from dose-response curves obtained by nonlinear regression analysis. Dose-response curves obtained for the compounds are represented and compared in Fig. 4.

As demonstrated by the IC_{50} values compiled in Table 3, the molybdenum complexes **1**, **2**, **4** and **2T** are efficient cytotoxic agents against the in vitro growth of HeLa cells, exhibiting activities with IC_{50} values ranging from 12 to 118 μM. Compounds **3** and **3T** did not show significant antiproliferative effect. The latter are the binuclear complexes with the ligand **L3** bridging the two metal centers and their geometric features (see Fig. 1 for **3**) are probably not adequate for interaction with DNA. The effect of complexes **1** and **4** is similar, in agreement with the comparable size of the π-system in ligands 2-(2′-pyridyl)imidazole (**L1**), and 2,2′-bisimidazole (**L4**); on the other hand, the addition of a fused benzene ring (2-(2′-pyridyl)benzimidazole, **L2**) has a dramatic effect on the antiproliferative action of complexes **2** and **2T**, which increases by 8–10 times. In these complexes, the π-system can probably approach DNA more easily, since the complexes are small but carry a large ring.

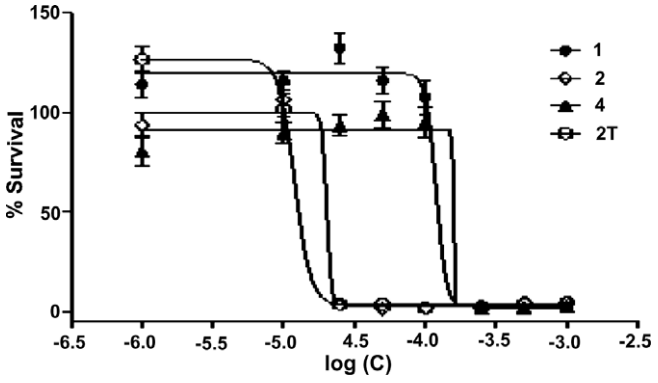

Fig. 4. Dose–response curves for compounds **1**, **2**, **4**, and **2T**. Compounds were tested in concentrations ranging from 1 to 1000 μM.

Table 3
IC_{50} of compounds against HeLa cells

Compounds	IC_{50} (μM)
1	118
2	15
3	>300
4	100
2T	12
3T	>300

Although the mechanisms of the antiproliferative activity of tested compounds are yet to be clarified, some introductory data suggest that apoptosis or other mechanisms leading to DNA degradation may be involved. In fact, the compounds were studied in respect to their binding behavior to DNA (salmon sperm DNA) by preliminary viscosity measurements and changes in specific viscosities upon the addition of compounds to DNA solution were not observed. Morphological cell analysis after staining with Hoechst 33342 reagent revealed the formation of apoptotic bodies. Further studies are necessary to explain the cytotoxicity of these molybdenum compounds against HeLa cells. The effects of the complexes against other cell lines will also be evaluated to check if the antiproliferative action has any cell specificity.

3. Conclusions

The complexes $[Mo(\eta^3\text{-}C_3H_5)Br(CO)_2(L)]$ with the bidentate nitrogen ligands 2-(2′-pyridyl)imidazole (**L1**), 2-(2′-pyridyl)benzimidazole (**L2**), N,N′-bis(2′-pyridinecarboxamido)-1,2-ethane (**L3**), and 2,2′-bisimidazole (**L4**) were prepared and characterized (L = **L1**, **1**; **L2**, **2**; **L4**, **4**). The binuclear complex $[\{Mo(\eta^3\text{-}C_3H_5)Br(CO)_2\}_2(\mu\text{-}\mathbf{L3})]$ (**3**), formed from reaction with **L3**, was structurally characterized by single crystal X-ray diffraction, which showed the presence of the axial isomer. Complexes **2** and **3** reacted with thallium triflate, leading to complexes **2T** and **3T** where bromide was substituted by the triflate ion. The molecules of **2T** assembled in a O···H–N hydrogen bonded dimer in the crystal structure.

The catalytic activity of these species as precursors for alkene oxidation in the presence of TBHP was tested, in order to compare the effect of changing the nitrogen ligands on this system [12]. The conversions are only moderate and the turnover frequencies vary between 175 and 82 mol mol_{Mo}^{-1} h^{-1} for styrene, and 159 and 75 mol mol_{Mo}^{-1} h^{-1} for cyclooctene, for complexes **1–3**. Complex **4** is a very poor precursor for these reactions. In the work reported earlier [12], efficient catalysts were obtained from complexes containing 1,4-(R-2,3-dimethyldiazabutadiene) (DAB) or 1,4-(4-R)phenyl-2,3-(1,9-naphtalene)diazabutadiene (BIAN) ligands, with 100% conversions in several examples, and a similar conversion in the second run, after another substrate load. The ligands used in the new complexes have one (**1–3**) or two (**4**) non coordinated N–H groups, which may be important in the reaction. Indeed, the ROOH peroxide may become involved in hydrogen bonds with the N–H group(s) of the ligands, making the formation of the active intermediate slower. The fact that complex **4**, bearing the 2,2′-bisimidazole (**L4**) ligand with two N–H, is a much worse catalyst precursor that the other three complexes supports this idea.

The molybdenum complexes **1**, **2**, **4**, and **2T** are efficient cytotoxic agents against the in vitro growth of HeLa cells, exhibiting activities with IC_{50} values ranging from 12 to 118 μM, while complexes **3** and **3T** display no antiproliferative action. In particular, the two complexes **2** and **2T** bearing the 2-(2′-pyridyl)benzimidazole ligand display an activity comparable to that of patented compounds and are therefore very promising.

4. Experimental

4.1. General considerations

All air-sensitive reactions and manipulations were performed using standard Schlenk techniques under an oxygen-free and water-free nitrogen atmosphere.

2-(2′-pyridyl)benzimidazole (**L2**), picolinic acid, ethylenediamine, allyl bromide, pyridine-2-aldehyde, cis-cyclooctene, styrene, dibutylether, glyoxal (40% water), and *t*-butylhydroperoxide (5.0–6.0 M in decane) were obtained from Aldrich, molybdenum hexacarbonyl from Fluka, and all solvents were purchased from standard chemical suppliers. Solvents were dried by standard procedures (THF, *n*-hexane and Et_2O over Na/benzophenone ketyl, CH_2Cl_2 and NCMe over CaH_2), distilled under nitrogen, and kept over 4 Å molecular sieves (3 Å for NCMe). Complexes [Mo(η^3-C_3H_5)Br$(CO)_2(CH_3CN)_2$] (**5**) were prepared following the synthetic procedure reported by tom Dieck et al. [6b], the ligands 2-(2′-pyridyl)imidazole (**L1**) [21] and 2,2′-bisimidazole (**L4**) [22], and thallium triflate from literature procedures [23].

Infrared spectra were recorded on a Unican Mattson Mod 7000 FTIR spectrophotometer as KBr pellets. ^{1}H and ^{13}C solution NMR spectra were obtained with a Bruker Avance-400 spectrometer. Chemical shifts are quoted in parts per million (ppm) from TMS. Microanalyses for C, H, and N were performed at the University of Vigo.

High resolution mass spectra (HR-MS) were performed at the Faculty of Science of the University of Lisbon in a ApexQe FTICR Mass Spectrometer from Bruker Daltonics (Billerica, MA, USA) equipped with an electrospray ion source (ESI) and a 7 T actively shielded superconducting magnet. The samples were introduced with a flow rate of 120 μL/h. The vacuum was maintained by means of mechanical vacuum pumps followed by turbomolecular pumps in two different regions: ion source (maintained $\sim 6.0 \times 10^{-6}$ mbar) and cell region (maintained $\sim 4.0 \times 10^{-10}$ mbar). The mass spectrometer was calibrated with a solution containing a mixture of polyethylenglycol (2.8×10^{-6} M) and ultramark (2.8×10^{-6} M) polymers in HPLC grade methanol and acidified with 0.1% (V/V) of acetic acid.

The mass spectra were acquired in the positive ion broadband mode, with an acquisition size of 512k, in the mass range of 50–1000. The nebulizer gas flow rate was set to 2.5 L/min, and the dry gas flow rate to 4.0 L/min at a temperature of 220 °C. The capillary voltage was set to 5000 V and the spray shield voltage to 4500 V. The ion source optics, collision cell, and ICR cell parameters were optimized to ensure the highest abundance possible for the ions of interest. All mass spectra recorded are the average of 16 mass spectra. The ions were accumulated in the collision cell during 1.5 s prior to their transfer to the ICR cell.

4.2. Preparation of N,N′-bis(2′-pyridinecarboxamido)-1,2-ethane (*L3*)

A solution of picolinic acid (6.15 g, 0.05 mol) and ethylenediamine (1.7 ml, 0.025 mol), in 2:1 ratio, was heated at 155 °C during 4 h. The orange oil formed was distilled at atmospheric pressure. The distillation started at 115 °C and was ended when the temperature started to drop. The solid residue was recrystallized in acetone/ether.

Yield: 65%. Anal. Calc. for $C_{14}H_{14}N_4O_2$: C, 62.24; H, 5.18; N, 20.74. Found: C, 59.46; H, 4.94; N, 19.92%.

IR (KBr, ν/cm^{-1}): 3331 (s), 3066 (m), 2942 (m), 1656 (s), 1589 (m), 1571 (m), 1531 (s), 1465 (m), 1432 (m), 1327 (m), 1290 (s), 1255 (s), 1231 (m), 1164 (m), 1086 (m), 1046 (m), 1029 (m), 995 (s), 967 (m), 888 (s), 819 (s), 748 (s), 677 (s), 620 (s), 493 (m), 448 (m), 404 (m).

*^{1}H NMR (400.*10 MHz, *$CDCl_3$, r.t., δ ppm)*: 3.76 (t, 4H, H7/H7′), 7.42 (t, 2H, H4/H4′), 7.84 (t, 2H, H3/H3′), 8.19 (d, 2H, H2/H2′), 8.41 (s, H, NH), 8.56 (d, 2H, H5/H5′). *^{13}C NMR (100.*25 MHz, *$CDCl_3$, r.t., δ ppm)*: 39.2 (C7/C7′), 121.9 (C2/C2′), 125.9 (C4/C4′), 137.0 (C3/C3′), 147.8 (C5/C5′), 149.4 (C1/C1′), 164.7 (C6/C6′).

HR ESI-MS (*m*/*z*): calcd for $[C_{14}H_{14}O_2N_4+K]^+$, 309.07483; obsd, 309.07563; error, +2.6; sigma, 0.0193.

4.3. Preparation of [Mo(η^3-C_3H_5)Br$(CO)_2$(*L1*)] (*1*)

A solution of 2-(2′-pyridyl)imidazole (**L1**) (0.15 g, 1 mmol) in dichloromethane was added to a solution of [Mo(η^3-C_3H_5)Br$(CO)_2(NCMe)_2$] (**5**) (0.36 g, 1 mmol) in dichloromethane, in 1:1 ratio. The mixture was stirred for one day, in inert atmosphere. The brown solid formed was filtered, washed with dichloromethane and diethyl ether, and dried under vacuum.

Yield: 52%. Anal. Calc. for $MoBrC_{13}H_{12}N_3O_2 + 0.5CH_2Cl_2$: C, 35.21; H, 2.84; N, 9.12. Found: C, 35.59; H, 2.81; N 9.80%.

IR (KBr, ν/cm^{-1}): 3430 (w), 3160 (w), 3130 (w), 3060 (m), 3000 (w), 2940 (w), 1940 (s), 1840 (s), 1660 (w), 1620 (s), 1570 (w), 1500 (w), 1470 (s), 1390 (w), 1290 (w), 1260 (w), 1160 (m), 1110 (m), 1090 (w), 1030 (w), 964 (w), 933 (w), 852 (w), 792 (s), 751 (s), 699 (s), 634 (w), 621 (w), 580 (w), 511 (w), 496 (w), 473 (w), 428 (w).

*^{1}H NMR (400.*10 MHz, *MeOD, r.t., δ ppm)*: 1.43 (m, H, η^3-C_3H_5), 1.58 (t, H, η^3-C_3H_5), 3.60 (m, 2H, η^3-C_3H_5), 4.10 (m, H, η^3-C_3H_5), 5.50 (s, H, CH_2Cl_2), 7.60 (s, 2H, H4/H5), 7.79 (s, H, H5′), 7,98 (s, H, H4′), 8.11 (d, H, H3′), 8.28 (t, H, H6′), 8.93 (s, H, NH). *^{13}C NMR (100.25 MHz, MeOD, r.t., δ ppm)*: 74.5 (η^3-C_3H_5), 121.0 (C5′/C6′), 122.0 (C4/C5), 126.0 (C3′), 141.0 (C4′).

4.4. Preparation of [Mo(η^3-C_3H_5)Br$(CO)_2$(*L2*)] (*2*)

A solution of 2-(2′-pyridyl)benzimidazole (**L2**) (0.20 g, 1 mmol) in dichloromethane, was added to a solution of [Mo(η^3-C_3H_5)Br$(CO)_2(NCMe)_2$] (**5**) (0.36 g, 1 mmol) in dichloromethane, in 1:1 ratio. The mixture was stirred for three days, in inert atmosphere. The red solid formed was filtered, washed with dichloromethane and diethyl ether, and dried under vacuum.

Yield: 81%. Anal. Calc. for $MoBrC_{17}H_{14}N_3O_2$: C, 43.61; H, 3.01; N, 8.98. Found: C, 43.1; H, 3.08; N, 8.89%.

IR (KBr, ν/cm^{-1}): 3854 (w), 3423 (w), 3107 (s), 3062 (s), 2976 (w), 2917 (w), 2368 (w), 2333 (w), 1934 (s), 1853 (s), 1602 (m), 1539 (m), 1478 (m), 1441 (s), 1381 (m), 1320 (m), 1298 (m), 1254 (m), 1148 (m), 982 (m), 818 (m), 744 (s), 665 (m), 629 (m), 604 (m), 571 (m), 496 (m), 463 (m), 434 (m).

*^{1}H NMR (400.*10 MHz, *DMF, r.t., δ ppm)*: 1.28 (d, H, η^3-C_3H_5), 1.40 (d, H, η^3-C_3H_5), 3.24 (m, H, η^3-C_3H_5), 3.30 (m, H, η^3-C_3H_5), 3.38 (m, H, η^3-C_3H_5), 7.53 (m, 2H, H5/H6), 7.73 (t, H, H4′), 7.79 (d, H, H7), 7.88 (d, H, H4), 8.29 (t, H, H5′), 8.51 (d, H, H6′), 8.94 (d, H, H3′). *^{13}C NMR (100.25 MHz, DMF, r.t., δ ppm)*: 52.8 (η^3-C_3H_5), 55.4 (η^3-C_3H_5), 73.5 (η^3-C_3H_5), 114.0 (C7), 119.0 (C4), 123.3 (C6′), 125.0 (C5), 126.1 (C6), 127.0 (C4′), 135.2 (C8), 140.0 (C5′), 141.3 (C9), 147.0 (C2), 151.3 (C1′), 153.5 (C3′).

4.5. Preparation of [{MoBr(η^3-C_3H_5)$(CO)_2$}$_2$(μ-*L3*)] (*3*)

A solution of *N*,*N*′-bis(2′-pyridinecarboxamido)-1,2-ethane (**L3**) (0.14 g, 0.5 mmol) was added to a solution of [Mo(η^3-C_3H_5)Br$(CO)_2(NCMe)_2$] (**5**) (0.36 g, 1 mmol) in dichloromethane, in 1:2 ratio. The mixture was stirred for three days, in inert atmosphere.

The dark red solid formed was filtered, washed with dichloromethane and diethyl ether, and dried under vacuum. *n*-Hexane

was added to the remaining solution, and another batch of red crystals was obtained. Some of these crystals were suitable for X-ray diffraction studies.

Yield: 65%.

IR (KBr, ν/cm^{-1}): 3265 (s), 3097 (m), 2992 (w), 1928 (s), 1857 (s), 1824 (s), 1630 (s), 1600 (s), 1556 (s), 1469 (s), 1432 (m), 1362 (m), 1341 (m), 1301 (m), 1264 (m), 1229 (w), 1183 (w), 1164 (w), 1105 (w), 1066 (m), 1019 (m), 997 (w), 961 (w), 905 (m), 850 (w), 804 (m), 747 (s), 688 (m), 633 (m), 606 (m), 570 (m), 558 (m), 493 (m), 479 (m), 444 (m), 419 (m).

*^{1}H NMR (400.*10 MHz, *CDCl$_3$, r.t., δ ppm):* 1.22 (t, 2H, η^3-C_3H_5), 1.53 (t, 2H, η^3-C_3H_5), 3.45 (m, 4H, η^3-C_3H_5), 3.56 (t, 2H, H7/H7′), 3.72 (t, 2H, H7/H7′), 3.94 (s, 2H, η^3-C_3H_5), 4,12 (s, 2H, η^3-C_3H_5), 7.65 (t, 2H, H4/H4′), 7.84 (t, 2H, H3/H3′), 8.02 (d, 2H, H2/H2′), 8.78 (s, H, NH), 9.47 (s, 2H, H5/H5′). *^{13}C NMR (100.*25 MHz, *CDCl$_3$, r.t., δ ppm):* 15.5 (η^3-C_3H_5), 37.3 (C7/C7′), 53.7 (CH_2Cl_2), 56.6 (η^3-C_3H_5), 75.2 (η^3-C_3H_5), 124.5 (C2/C2′), 128.8 (C4/C4′), 139.6 (C3/C3′), 146.4 (C1/C1′), 154.2 (C5/C5′), 169.8 (C6/C6′).

HR ESI-MS (*m*/*z*): calcd for [$Mo_2BrC_{24}H_{24}O_6N_4^+ - Br$], 738.89824; obsd, 738.90328; error, +2.6; sigma, 0.0191.

4.6. Preparation of [Mo(η^3-C_3H_5)Br(CO)$_2$(**L4**)] (**4**)

A solution of 2,2′-bisimidazole (**L4**) (0.13 g, 1 mmol) was added to a solution of [Mo(η^3-C_3H_5)Br(CO)$_2$(NCMe)$_2$] (**5**) (0.36 g, 1 mmol) in dichloromethane, in 1:1 ratio. The mixture was stirred for one day, in inert atmosphere. The yellow solid formed was filtered, washed with dichloromethane and diethyl ether, and dried under vacuum.

Yield: 80%. Anal. Calc. for $MoBrC_{11}H_{11}N_4O_2$: C, 32.46; H, 2.72; N, 13.76. Found: C, 31.585; H, 2.775; N, 13.695%.

IR (KBr, ν/cm^{-1}): 3250 (m), 3163 (s), 2993 (m), 2362 (w), 2337 (w), 1931 (s), 1833 (s), 1629 (m), 1528 (s), 1499 (m), 1458 (w), 1422 (s), 1382 (m), 1316 (s), 1176 (s), 1132 (s), 1099 (s), 1090 (s), 1028 (m), 763 (s), 746 (s), 683 (s), 619 (m), 493 (m), 474 (m).

^{1}H NMR (400.10 MHz, MeOD r.t., δ ppm): 1.3 (s, 2H, η^3-C_3H_5), 3.4 (s, 2H, η^3-C_3H_5), 4.0 (s, H, η^3-C_3H_5), 5.4 (s, 2H, CH_2Cl_2), 7.2 (s, 2H), 7.4 (s, 2H), 7.6 (s, 2H, NH). *^{13}C NMR (100.*25 MHz, *MeOD, r.t., δ ppm):* 57.6 (η^3-C_3H_5), 73.7 (η^3-C_3H_5), 121.9 (C).

HR ESI-MS (*m*/*z*): calcd for [$MoC_{11}H_{11}O_2N_4^+ - Br$], 328.99322; obsd 328.99579; error, +8.3; sigma, 0.0785.

4.7. Preparation of [Mo(η^3-C_3H_5)(CF_3SO_3)(CO)$_2$(**L2**)] (**2T**)

A solution of thallium triflate ($TlCF_3SO_3$) (0.18 g, 0.5 mmol) in dichloromethane was added to a solution of [MoBr(η^3-C_3H_5)(CO)$_2$(**L2**)] (**2**) (0.24 g, 0.5 mmol) in acetonitrile, in 1:1 ratio. There was an immediate reaction with the formation of a white solid (TlBr). After two hours under reflux, the solution was filtered with celite and diethyl ether was added. After a few days it started to form an orange solid that was filtered and washed with diethyl ether and dried under vacuum. Crystals suitable for X-ray diffraction studies were obtained by recrystallizing the solid from dichloromethane/*n*-hexane.

Yield: 59%. Anal. Calc. for $MoC_{18}H_{13}N_3O_5F_3S$: C, 40.32; H, 2.42; N, 7.84; S, 5.98. Found: C, 39.8; H, 2.5; N, 7.8; S 6.8%.

IR (KBr, ν/cm^{-1}): 3134 (m), 3005 (m), 2936 (m), 1948 (s), 1865 (s), 1607 (s), 1488 (s), 1457 (s), 1447 (m), 1324 (w), 1308 (w), 1259 (s), 1285 (s), 1226 (s), 1208 (s), 1179 (s), 1022 (s), 987 (m), 792 (m), 763 (m), 745 (s), 631 (s), 582 (m), 519 (m), 508 (m).

*^{1}H NMR (400.*10 MHz, *MeOD r.t., δ ppm):* 1.30 (d, H, η^3-C_3H_5), 1.40 (d, H, η^3-C_3H_5), 3.02 (m, H, η^3-C_3H_5), 3.38 (m, 2H, η^3-C_3H_5), 3.58 (m, H, η^3-C_3H_5), 3.83 (m, H, η^3-C_3H_5), 4.25 (m, 2H, η^3-C_3H_5), 7.56–7.83 (m, 4H, H5′/H6′/H4/H7′), 8.03 (d, H, H4′), 8.25 (m, H, H5), 8.70 (d, H, H6), 8.90 (s, H, NH), 9.10 (d, H, H3). *^{13}C NMR (100.*25 MHz, *MeOD, r.t., δ ppm):* 56.5 (η^3-C_3H_5), 57.8 (η^3-C_3H_5), 74.1 (η^3-C_3H_5), 114.6 (C7′), 119.3 (C4′), 124.0 (C6), 126.6 (C5′), 127.6 (C6′), 128.8 (C4), 135.9 (C8′), 142.1 (C5), 144.2 (C9′), 147.9 (C2′), 150.9 (C1), 152.6 (C3).

4.8. Preparation of [{Mo(η^3-C_3H_5)(CF_3SO_3)(CO)$_2$}$_2$(μ-**L3**)] (**3T**)

A solution of thallium triflate ($TlCF_3SO_3$) (0.35 g, 1 mmol) in dichloromethane was added to a solution of [{MoBr(η^3-C_3H_5)(CO)$_2$}$_2$(μ-**L3**)] (**3**) (0.21 g, 0.5 mmol) in acetonitrile, in 2:1 ratio. There was an immediate reaction with the formation of a white solid. After 2 h under reflux, the solution was filtered with celite and diethyl ether was added. Red crystals started to form after a few days. They were filtered, washed with diethyl ether, and dried under vacuum.

Yield: 64%. Anal. Calc. for $MoC_{20}H_{19}N_4O_7F_3S$: C, 32.72; H, 2.52; N, 5.87; S, 6.72. Found: C, 31.58; H, 2.57; N, 6.27; S, 5.92%.

IR (KBr, ν/cm^{-1}): 3351 (s), 3111 (m), 2997 (m), 2957 (w), 2358 (w), 1949 (s), 1853 (s), 1636 (s), 1604 (s), 1561 (s), 1475 (s), 1445 (m), 1406 (w), 1367 (m), 1345 (s), 1291 (s), 1225 (s), 1182 (s), 1069 (w), 1030 (s), 971 (w), 926 (w), 908 (w), 808 (m), 740 (m), 710 (w), 688 (w), 632 (s), 574 (m), 562 (w), 514 (m), 497 (w), 475 (w), 446 (w), 418 (w).

*^{1}H NMR (400.*10 MHz, *CDCl$_3$, r.t., δ ppm):* 1.71 (d, 2H, η^3-C_3H_5), 3.46–3.69 (m, 4H, H7/H7′), 3.77(s, 2H, η^3-C_3H_5), 3.96 (s, 2H, η^3-C_3H_5), 4.17 (m, 2H, η^3-C_3H_5), 7.83 (t, 2H, H4/H4′), 7.88 (d, 2H, H2/H2′), 8.03 (t, 2H, H3/H3′), 8.91 (s, 2H, NH), 9.68 (s, 2H, H5/H5′). *^{13}C NMR (100.*25 MHz, *DMF, r.t., δ ppm):* 38.0 (C7/C7′), 60.0 (η^3-C_3H_5), 63.5 (η^3-C_3H_5), 73.0 (η^3-C_3H_5), 123.6 (C2/C2′), 128.8 (C4/C4′), 140.0 (C3/C3′), 154.4 (C5/C5′).

HR ESI-MS (*m*/*z*): calcd for [$Mo_2C_{25}H_{24}O_9N_4F_3S^+ - CF_3SO_3$], 808.93318; obsd, 808.94041; error, 7.1; sigma, 0.0177.

4.9. Catalytic epoxidation of cyclooctene and styrene in the presence of 1-4 with TBHP

Cyclooctene (7.3 mmol) or styrene (7.7 mmol) and *t*-butylhydroperoxide (200 mol%, 5.5 M solution in decane) were mixed in the presence of complexes **1–4** (1 mol%) in a glass reactor, at 55 °C, and vigorously stirred. The reaction was monitored by taking samples at specific reaction times and analyzing them by gas chromatography (GC), using an Agilent 6890 Series gas chromatograph, equipped with an Agilent 7683 automatic liquid sampler and coupled to an Agilent 5973*N* mass selective detector (MSD) (Agilent Technologies, Little Falls, DE, USA). The GC analyses were performed on a TRB-5MS (30 m × 0.25 mm ID × 0.25 μm film thickness) capillary column (5% diphenyl, 95% dimethylpolysiloxane; Teknokroma S. Coop. C. Ltd., Barcelona, Spain) and helium was used as carrier gas maintained in the constant pressure mode (7.36 psi). The oven temperature was programmed from 60 °C (held for 3 min) to 200 °C (held for 2 min) at 10 °C/min. The inlet was set at 250 °C operating with a split ratio of 25:1 and 1 μL of each sample was injected. The transfer line, ion source and quadrupole analyzer temperatures were maintained at 280, 230 and 150 °C, respectively, and a solvent delay of 3 min was selected. The mass selective detector operated in the full-scan mode acquisition and electron ionization mass spectra in the range 35–550 Da were recorded at 70 eV electron energy with an ionization current of 34.6 μA. Data analysis and instrument control were performed by the MSD CHEMSTATION software (G1701CA; version C.00.00; Agilent Technologies). For the determination of the conversion percentages, the ratio of the abundance areas of olefins and the internal standard (DBE) was calculated.

Table 4
Crystal data and refinement details for complexes **3** and **2T**

Compound	**3**	**2T**
Empirical Formula	$C_{26}H_{26}Br_2Mo_2N_2O_6$	$C_{18}H_{14}F_3MoN_3O_5S$
M_w	816.17	537.31
Crystal system	Monoclinic	Monoclinic
Space group	$C2/c$	$P2_1/c$
a (Å)	11.506(9)	10.032(9)
b (Å)	27.989(13)	12.062(11)
c (Å)	12.896(15)	17.66(2)
β (°)	101.75(10)	93.13(10)
V (Å^3)	4066(6)	2134(4)
Z	4	4
D_c (mg m^{-3})	1.333	1.673
μ (mm^{-1})	2.613	0.773
Reflections collected	12948	14316
Unique reflections [$R_{(int)}$]	3795 [0.0783]	3968[0.0484]
Final R indices		
R_1, wR_2 [$I > 2\sigma I$]	0.0854, 0.1617 [3159]	0.0667, 0.1252 [3478]
R_1, wR_2 (all data)	0.1108, 0.1753	0.0778, 0.1288

4.10. Crystallography

X-Ray data were collected at 298 K on a Marresearch Image Plate diffractometer with graphite monochromatized (Mo Kα radiation λ = 0.71073 Å) at Reading University. The crystals were positioned at 70 mm from the Image Plate and the frames were measured using a counting time of 2 m. Data analyses were carried out with the XDS program [24]. Empirical absorption corrections were carried out using the DIFABS program [25].

The structures were solved by direct methods and by subsequent difference Fourier syntheses and refined by full matrix least squares on F^2 using the SHELX-97 system programs [26]. Anisotropic thermal parameters were used for all non-hydrogen atoms. Hydrogen atoms bonded to the carbon and nitrogen atoms were included in refinement in calculated positions with the exception of the hydrogen atoms of the amide group of **3**, which were located from difference Fourier map and refined with N–H constrained distance. The atomic positions of all hydrogen atoms were refined with isotropic parameters equivalent 1.2 times those of the atom to which they are attached. Molecular diagrams presented are drawn with PLATON software [27]. Crystal data together with selected refinement parameters are listed in Table 4.

4.11. Biological studies

Cells: HeLa were grown at 37 °C in a 5% CO_2 atmosphere in RPMI 1640 medium, supplemented with 10% foetal calf serum (FCS), 2×10^{-3} mol dm^{-3} glutamine and 50×10^{-6} g ml^{-1} penicillin.

Compounds were dissolved in DMSO and tested in concentrations ranging from 1 to 1000 μM in the final medium.

Cytotoxicity assays: cell cultures were exposed for 48 h to different concentrations of compounds to be tested. UV–Vis spectra of solutions with appropriate concentrations were measured during this period and showed no decomposition of the compounds being studied. Cytotoxicity of test compound was evaluated by the MTT method [28]. The optical density was measured at 530 nm using a 96-well multiscanner autoreader. The IC_{50} values were calculated by non linear regression analysis using the graphed Prism software (GRAPHPAD Software, Inc., San Diego, California).

Supplementary material

CCDC 689473 and 689473 contain the supplementary crystallographic data for **3** and **2T**, respectively. These data can be obtained free of charge from The Cambridge Crystallographic Data Centre via www.ccdc.cam.ac.uk/data_request/cif.

Acknowledgements

S.Q. and F.C.M.P thank Fundação para a Ciência e a Tecnologia (Portugal) for fellowships (SFRH/BPD/11463/2002 and SFRH/BD/24598/2005, respectively). We thank Dr. P.D. Vaz for the MS experiments.

References

[1] (a) C. Thurier, P. Doppelt, Coord. Chem. Rev. 252 (2008) 155–169;
(b) V.A. Friese, D.G. Kurth, Coord. Chem. Rev. 252 (2008) 199–211;
(c) M.W. Cooke, D. Chartrand, G.S. Hanan, Coord. Chem. Rev. 252 (2008) 903–921.
[2] (a) K.H. Thompson, C. Orvig, Dalton Trans. (2006) 761–764;
(b) T. Storr, K.H. Thompson, C. Orvig, Chem. Soc. Rev. 35 (2006) 534–544.
[3] (a) V. Ritleng, M.J. Chetcuti, Chem. Rev. 107 (2007) 797–858;
(b) L. Yin, J. Liebscher, Chem. Rev. 107 (2007) 133–173.
[4] H.-U. Blaser, A. Indolese, A. Schnyder, Curr. Sci. 78 (2000) 1336–1344.
[5] (a) Y. Yamaguchi, K. Ogata, K. Kobayashi, T. Ito, Dalton Trans. (2004) 3982–3990;
(b) P.K. Baker, Adv. Organomet. Chem. 40 (1996) 45.
[6] (a) R.G. Hayter, J. Organometal. Chem. 13 (1968) Pl–P3;
(b) H. tom Dieck, H. Friedel, J. Organomet. Chem. 14 (1968) 375–385.
[7] D. Morales, J. Pérez, L. Riera, V. Riera, R. Corzo-Suárez, S. García-Granda, D. Miguel, Organometallics 21 (2002) 1540–1545.
[8] V.S. Joshi, M. Nandi, H. Zhang, B.S. Haggerty, A. Sarkar, Inorg. Chem. 32 (1993) 1301–1303.
[9] (a) B.M. Trost, M. Lautens, J. Am. Chem. Soc. 104 (1982) 5543–5545;
(b) B.M. Trost, M. Lautens, J. Am. Chem. Soc. 109 (1987) 1469–1478;
(c) B.M. Trost, C.A. Merlic, J. Am. Chem. Soc. 112 (1990) 9590–9600.
[10] Y. Yamaguchi, A. Fujita, N. Suzuki, T. Ito, J. Mol. Catal. A: Chem. 240 (2005) 226–232.
[11] J.W. Goodyear, C.W. Hemingway, R.W. Harrington, M.R. Wiseman, B.J. Brisdon, J. Organomet. Chem. 664 (2002) 176–181.
[12] J.C. Alonso, P. Neves, M.J. Pires da Silva, S. Quintal, P.D. Vaz, C. Silva, A.A. Valente, P. Ferreira, M.J. Calhorda, V. Félix, M.G.B. Drew, Organometallics 26 (2007) 5548–5556.
[13] (a) J.-M. Brégeault, Dalton Trans. (2003) 3289–3302;
(b) K.A. Jørgensen, Chem. Rev. 89 (1989) 431–458.
[14] (a) M.K. Trost, R.G. Bergman, Organometallics 10 (1991) 1172–1178;
(b) A.M. Martins, C.C. Romão, M. Abrantes, M.C. Azevedo, J. Cui, A.R. Dias, M.T. Duarte, M.A. Lemos, T. Lourenço, R. Poli, Organometallics 24 (2005) 2582–2589;
(c) A.A. Valente, J.D. Seixas, I.S. Gonçalves, M. Abrantes, M. Pillinger, C.C. Romão, Catal. Lett. 101 (2005) 127–130.
[15] M. Abrantes, A.M. Santos, J. Mink, F.E. Kühn, C.C. Romão, Organometallics 22 (2003) 2112–2118.
[16] (a) J.R. Ascenso, C.G. de Azevedo, M.J. Calhorda, M.A.A.F. de C.T. Carrondo, P. Costa, A.R. Dias, M.G.B. Drew, A.M. Galvão, C.C. Romão, V. Félix, J. Organomet. Chem. 632 (2001) 197–208;
(b) P.M.F.J. Costa, M. Mora, M.J. Calhorda, V. Félix, P. Ferreira, M.G.B. Drew, H. Wadepohl, J. Organomet. Chem. 687 (2003) 57–68;
(c) P.N. Martinho, S. Quintal, P. Costa, S. Losi, V. Félix, M.C. Gimeno, A. Laguna, M.G.B. Drew, P. Zanello, M.J. Calhorda, Eur. J. Inorg. Chem. (2006) 4096–4103.
[17] (a) M.N. Matos, C. Pereira, S. Rodrigues, M.J.P. da Silva, M. Mora, P. Alves, C.A. Reis, C.C. Romão, Patent Organometallic Molybdenum Compounds for Treating Cancer, WO 2005/087783 A1;
(b) S. Quintal, J. Matos, I. Fonseca, V. Félix, M.G.B. Drew, N. Trindade, M. Meireles, M.J. Calhorda, Inorg. Chim. Acta 361 (2008) 1584–1596.
[18] (a) S. Trofimenko, Inorg. Chem. 11 (1970) 2493–2499;
(b) D.R. Van Staveren, E. Bill, E. Bothe, M. Bühl, T. Weyhermüller, N. Metzler-Nolte, Chem. Eur. J. 8 (2002) 1649–1662;
(c) P. Espinet, R. Hernando, G. Iturbe, F. Villafañe, A.G. Orpen, I. Pascual, Eur. J. Inorg. Chem. (2000) 1031–1038.
[19] (a) R.H. Fenn, A.J. Graham, J. Organomet. Chem. 37 (1972) 137–150;
(b) D. Morales, M.E. Navarro Clemente, J. Pérez, L. Riera, V. Riera, D. Miguel, Organometallics 21 (2002) 4934–4938.
[20] (a) F.E. Kühn, M. Groarke, E. Bencze, E. Herdtweck, A. Prazeres, A.M. Santos, M.J. Calhorda, C.C. Romão, I.S. Gonçalves, A.D. Lopes, M. Pillinger, Chem. Eur. J. 8 (2002) 2370–2383;
(b) L.F. Veiros, A. Prazeres, P.J. Costa, C.C. Romão, F.E. Kühn, M.J. Calhorda, Dalton Trans. (2006) 1383–1389.
[21] B. Chiswell, F. Lions, B.S. Morris, Inorg. Chem. 3 (1964) 110–114.
[22] H. Debus, Ann. 107 (1859) 199–208.
[23] J. Vicente, M.-T. Chicote, M.M. Alvarez-Falcón, Organometallics 23 (2004) 5707–5712.
[24] W. Kabsch, J. Appl. Cryst. 21 (1988) 916–932.
[25] N. Walker, D. Stuart, Acta Crystallogr. Sect. A 39 (1983) 158–166.
[26] G.M. Sheldrick, SHELX-97, University of Göttingen, Göttingen, Germany, 2007.
[27] A.L. Spek, PLATON, A Multipurpose Crystallographic Tool, Utrecht University, Utrecht, The Netherlands, 2008.
[28] T. Mossman, J. Immunol. Meth. 65 (1983) 55–63.